J. Fluid Mech. (1981), *vol.* 113, *pp.* 269–282
Printed in Great Britain

Several plume flows in pure and saline water at its density extremum

By J. C. MOLLENDORF, R. S. JOHNSON† AND B. GEBHART‡

Department of Mechanical Engineering, State University of New York at Buffalo, Amherst, New York 14260

(Received 19 January 1979)

An accurate representation of the motion-causing buoyancy force, in the vicinity of the maximum-density condition in water at low temperatures, is determined by using a very accurate and quite simple equation of state for both pure and saline water. The resulting general laminar boundary-layer flow equations admit similarity solutions and, in the absence of salinity diffusion, require only one additional new dimensionless variable, called R. For flows of constant heat content in an unstratified ambient fluid, similarity is found only when the far-field temperature is at the temperature of maximum density. The three flow situations considered here are two above a horizontal line heat source and one above a point heat source. The first flow is a freely rising plane plume and the second is a wall plume (flow over a vertical, adiabatic surface with a horizontal line source imbedded in it). The third flow is the freely rising axisymmetric plume. These are the models in laminar theory of many processes which arise in cold water. A primary objective here is to calculate the effect of using a nonlinear density relation for water, which is much more accurate at low temperatures than the conventional linear one used in 'classical' analyses. The downstream variations of the temperature and velocity fields are found to be very different from those for flows where the effect of a density extremum is not included.

1. Introduction

A balance, at about 4 °C, of the competing density-controlling mechanisms of hydrogen bonding and molecular thermal motion result in a density extremum in pure water at atmospheric pressure. For circumstances in local thermodynamic equilibrium, an extremum also occurs in saline water at atmospheric pressure, up to a salinity level, s, of about 26 parts per thousand (‰), and at pressures up to about 300 bars abs. in pure water. For non-equilibrium conditions, a density extremum may also be found well beyond these limits.

Much of the natural surface water and some technological transport processes which involve low-temperature water occur within these ranges of temperature, salinity and pressure. When flows are driven by temperature and salinity gradients around the level of a density extremum, maximum density conditions may strongly influence

† Present address: Harrison Radiator Division, General Motors Corporation, Lockport, NY 14094.

‡ Present address: Department of Mechanical Engineering & Applied Mechanics, University of Pennsylvania, Philadelphia, PA 19104.

the resulting motion. Moreover, the large Lewis numbers associated with such phenomena, coupled with the dependence of density on temperature, salinity and pressure and the dependence of the temperature of inversion on both salinity and pressure may result in multiple extrema across a given flow region.

Convective motions in low-temperature pure water have received considerable attention in the past. External flows have been considered both experimentally and analytically, for spherical, cylindrical and flat surfaces. A minimum in heat transfer associated with convective reversal (or inversion) around the density extremum has been measured and predicted by several previous investigators as discussed by Bendell & Gebhart (1976) and Gebhart & Mollendorf (1978). Bendell & Gebhart (1976) measured the melting rate of vertical ice surfaces in pure water at temperatures ranging from about 2 °C to 20 °C. The results are converted to a heat-transfer parameter and are in very good agreement with the calculations of Gebhart & Mollendorf (1978).

At first, a general analysis of such flow encounters considerable complications. The first part of the conventional Oberbeck–Boussinesq approximation is applicable inasmuch as density variation may be neglected in continuity considerations. Difficulty arises, however, because of the motion-causing buoyancy force $\mathbf{g}(\rho_r - \rho)$, where $\mathbf{g}$ is gravity and $\rho(t, s, p)$ is the local density. The local reference density, ρ_r, is usually taken to be that which determines the local hydrostatic pressure level p_h. The second part of the Oberbeck–Boussinesq approximation is the expression of this local density difference as a linear function of the differences in the motion-causing driving force, $(t - t_r)$ and $(s - s_r)$. Such a formulation was used by Gebhart & Pera (1971) and Pera & Gebhart (1972), but it is not reasonable when a density extremum condition arises, since the volumetric coefficient of thermal expansion, β, may be positive, zero and negative within such a flow. The awkwardness of such a conventional approach is apparent from the ice-melting results and observations of Bendell & Gebhart (1976).

Therefore, instead of using the usual Oberbeck–Boussinesq approximation one is led to the direct use of a density relation in the buoyancy force. Past studies have encountered considerable problems: either accuracy has been sacrificed for simplicity in analysis or, with more accurate representation, many additional problem-dependent parameters have been generated.

Gebhart & Mollendorf (1977) have recently improved the possibilities for the direct use of a simple and accurate buoyancy-force formulation by developing a new density equation for both pure and saline water. It has very high accuracy to 20 °C, to a salinity, s, of 40‰ and to a pressure level, p, of 1000 bars abs. It accomplishes this with only one temperature term, in an expansion around the temperature of the density extremum, $t_m(s, p)$, at any particular values of s and p. The most accurate form has an r.m.s. difference of density of 3·5 p.p.m. with the pure water correlation of Fine & Millero (1973) and 10·4 p.p.m. with the Chen & Millero (1976) saline-water data. Another even more convenient result for analysis has corresponding r.m.s. differences of 6·5 and 38·2 p.p.m., respectively.

With this density formulation, Gebhart & Mollendorf (1978) have analysed boundary-region flows induced by thermal and saline diffusion, and with the two combined. They show that self-similarity results for a broad range of conditions, and give solutions for a number of thermally driven flows generated adjacent to a vertical surface, including ice melting and variable surface temperature. In the analysis the temperature effect arises only in the appearance of a new parameter R,

$$R = \frac{t_m(s_\infty, p) - t_\infty}{t_0 - t_\infty}. \tag{1}$$

The buoyancy force is taken, as in external flow, as $\mathbf{g}(\rho_\infty - \rho)$. Then, using the density relation of Gebhart & Mollendorf (1977), $\rho = \rho_m[1 - \alpha|t - t_m|^q]$, it was found, in the absence of saline diffusion, that

$$\begin{aligned} \rho_\infty - \rho &= \rho(t_\infty, s_\infty, p) - \rho(t, s_\infty, p) \\ &= \rho_m(s_\infty, p)\, \alpha(s_\infty, p) |t_0 - t_\infty|^q [|\phi - R|^q - |R|^q] \\ &\equiv \rho_m \alpha |t_0 - t_\infty|^q W, \end{aligned} \tag{2}$$

$$\phi \equiv \frac{t - t_\infty}{t_0 - t_\infty}, \tag{3}$$

where $W = W(\eta) \equiv |\phi - R|^q - |R|^q$ is the buoyancy force for the momentum equation in similarity form. The density at the extremum, ρ_m, as well as α, q and t_m are salinity and pressure dependent and follow from Gebhart & Mollendorf (1977). Note that $q = 1$ corresponds to the second part of the conventional Oberbeck–Boussinesq approximation. Otherwise, values of q range from about 1·6 to 1·9 for salinities to 35‰ and pressures to 1000 bar abs. The effects on density of motion pressure differences across the flow region are neglected; see the discussion in Gebhart & Mollendorf (1978) concerning pressure effects.

The present investigation uses the above formulation with boundary conditions corresponding to two plane flows arising from a horizontal line source of thermal energy and an axisymmetric flow resulting from a point thermal source. The two plane flows are the freely rising plane plume and the flow adjacent to an adiabatic surface with a horizontal line source imbedded in it. The other flow is the axisymmetric plume. We shall give the solutions for these flows in ambient water uniformly at its extremum density condition, that is at $t_\infty = t_m(s_\infty, p)$. This corresponds to $R = 0$, with flow and buoyancy upward, and is the only similarity condition for these plume flows in an unstratified ambient. Since these flows are thermally driven, no salinity gradients will arise, neglecting both the Sorét and Dufour effects. An estimate of the order of magnitude of the ratio of the Sorét term to a principal term in the mass diffusion equation, $S_T \nabla . [s(1-s)\nabla t]/\nabla^2 s \approx S_T s(1-s)\Delta t/\Delta s Le^2$, is calculated to be about 10^{-6}, where S_T is the Sorét coefficient and s, t and Le are salinity, temperature and the Lewis number, respectively. As explained by Caldwell (1974), the Dufour effect is negligible in liquids as a consequence of the Onsager relations.

To summarize, previous investigations of transport in water around its density extremum has been mainly for pure water at atmospheric pressure. Most previous analytical studies have employed the buoyancy-force approximation of Merk (1953) involving Chappius' density coefficients, or the other conventional one, $\alpha(\Delta t)^2$. Integral analysis has been used around the sphere and also adjacent to a vertical surface. A common simplification in previous analyses using the full equations has been to take $t_\infty = t_m$, the extremum temperature. This means, of course, that no buoyancy inversion occurs in the flow region and that the flow is always upward. Several previous studies have used a cubic polynomial for density variations with temperature which resulted in additional parameters beyond those of simpler density formulations. There is no known previous study of plume flows in low-temperature water with density extrema effects included.

The present work is a similarity analysis of three constant-buoyancy plume flows in pure or saline water at its extremum temperature. Although the effect of saline diffusion is neglected, the influence of salinity level is retained. The following analysis considers the only conditions for which a similarity solution is known for constant-buoyancy plume flows in cold unstratified water. The calculated results cover a wide range of Prandtl number and salinity and pressure levels.

2. Analysis

The equations of steady laminar motion, with the first of the Oberbeck–Boussinesq approximations, and constant fluid absolute viscosity, μ, and fluid thermal conductivity, k, are:

$$\nabla . \mathbf{w} = 0, \tag{4}$$

$$\rho_1(\mathbf{w} . \nabla)\,\mathbf{w} = \mathbf{g}(\rho_\infty - \rho) - \nabla p_m + \mu V^2 \mathbf{w}, \tag{5}$$

$$\rho_1 c_p(\mathbf{w} . \nabla)\,t = k\nabla^2 t + \beta T(\mathbf{w} . \nabla)\,p + \mu\Phi, \tag{6}$$

where p_m is the local motion pressure (i.e. the difference between the local static pressure and the local hydrostatic pressure), $\mathbf{w}$ is the local fluid velocity vector and Φ is the viscous dissipation term in the energy equation. The Sorét and Dufour effects are small for the flows considered here and have been neglected as explained above. Also, distributed thermal or salinity sources, as from reaction, are not included. It is assumed that the salinity, s, is usually a small component of the total density of saline water. For example, the salinity of estuary water could be about 20‰, that is 2·0% or 0·020 grams of solute to one gram of water. The viscous dissipation and pressure terms in (6) will be discarded later.

Taking x positive in the direction opposed to gravity and applying the boundary-layer approximations, we have (7), (8) and (9) below for plane flow and (10), (11) and (12) for axisymmetric flow, where y is normal to the x direction and outward into the flow region:

$$\frac{\partial u}{\partial x} + \frac{\partial v}{\partial y} = 0, \tag{7}$$

$$\rho_1\left(u\frac{\partial u}{\partial x} + v\frac{\partial u}{\partial y}\right) = \mu\frac{\partial^2 u}{\partial y^2} + g(\rho_\infty - \rho), \tag{8}$$

$$\rho_1 c_p\left(u\frac{\partial t}{\partial x} + v\frac{\partial t}{\partial y}\right) = k\frac{\partial^2 t}{\partial y^2} + \beta T u\frac{dp_h}{dx} + \mu\left(\frac{\partial u}{\partial y}\right)^2; \tag{9}$$

$$\frac{\partial}{\partial x}(yu) + \frac{\partial}{\partial y}(yv) = 0, \tag{10}$$

$$\rho_1\left(u\frac{\partial u}{\partial x} + v\frac{\partial u}{\partial y}\right) = \mu\frac{1}{y}\frac{\partial}{\partial y}\left(y\frac{\partial u}{\partial y}\right) + g(\rho_\infty - \rho), \tag{11}$$

$$\rho_1 c_p\left(u\frac{\partial t}{\partial x} + v\frac{\partial t}{\partial y}\right) = k\frac{1}{y}\frac{\partial}{\partial y}\left(y\frac{\partial t}{\partial y}\right) + \beta T u\frac{dp_h}{\partial x} + \mu\left(\frac{\partial u}{\partial y}\right)^2. \tag{12}$$

Saline diffusion is not considered here, but the effect of variable ambient salinity is included. The effect of motion pressure has been shown to be negligible by Gebhart & Mollendorf (1978), but the effect of variable ambient pressure is included. The apparent

boundary conditions are, respectively, for (*a*) the plane plume, (*b*) the adiabatic surface and (*c*) the axisymmetric plume

$$(a)\ v = \frac{\partial u}{\partial y} = \frac{\partial \phi}{\partial y} = 0 \quad \text{at} \quad y = 0, \quad u = \phi = 0 \quad \text{as} \quad y \to \infty; \tag{13a}$$

$$(b)\ v = u = \frac{\partial \phi}{\partial y} = 0 \quad \text{at} \quad y = 0, \quad u = \phi = 0 \quad \text{as} \quad y \to \infty; \tag{13b}$$

$$(c)\ v = \frac{\partial u}{\partial y} = \frac{\partial \phi}{\partial y} = 0 \quad \text{at} \quad y = 0, \quad u = \phi = 0 \quad \text{as} \quad y \to \infty. \tag{13c}$$

A transformation in terms of a similarity variable $\eta(x, y)$ and the usual stream functions $\psi(x, y)$ and $f(\eta)$ are defined following the notation of Gebhart (1971, 1973):

$$\eta = yb(x), \quad \psi(x, y) = \nu c(x) f(\eta), \quad t_0 - t_\infty = d(x). \tag{14}$$

Velocities are related in the usual way to the conventional stream function for the plane flows, and to the Stokes stream function for the axisymmetric plume. The fluid is unstratified, and the function d is the variation of temperature at $y = 0$.

The scaling functions b and c depend on the local vigour and extent of the flow and are to be determined. For a purely thermally driven flow, the local flow vigour is conventionally indicated by a local Grashof number defined as $Gr_x = (gx^3/\nu^2)\beta(t_0 - t_\infty)$. This incorporates the second part of the Oberbeck–Boussinesq approximation. In general, the Grashof number can be considered to be the 'unit Grashof number', gx^3/ν^2, times some measure of buoyancy, for example $\beta(t_0 - t_\infty)$. A conventional way to include additional buoyancy, due to species diffusion for example, is to include additional buoyancy of similar form. See, for example, Gebhart & Pera (1971) and Mollendorf & Gebhart (1974).

Around a density extremum, however, a single linear term is not an accurate estimate of the buoyancy force. A much more representative estimate of the motion-causing density difference must be used in $Gr_x = (gx^3/\nu^2)\Delta\rho/\rho$. We have found that a consistent and effective way to define buoyancy is in its overall effect, which is the integral I_w of W in equation (2) across the flow region.

Introducing the transformations (14) into (7), (8) and (9) and also into (10), (11) and (12), we have equations (15) and (16) for plane flow and (17) and (18) for axisymmetric flow:

$$f''' + \frac{c_x}{b} f f'' - \left(\frac{c_x}{b} + \frac{c b_x}{b^2}\right) f'^2 + \frac{g}{\nu^2 c b^3} \frac{(\rho_\infty - \rho)}{\rho_1} = 0, \tag{15}$$

$$\frac{\phi''}{Pr} + \frac{c_x}{b} f \phi' - \frac{c d_x}{b d} f' \phi - \beta T \frac{c}{b d} \frac{g}{c_p} f' + \frac{b^2 c^2}{d} \frac{\nu^2}{c_p} f''^2 = 0; \tag{16}$$

$$\frac{f'''}{\eta} - \frac{f''}{\eta^2} + \frac{f}{\eta^3} + c_x \left(\frac{f f''}{\eta^2} - \frac{f f'}{\eta^3}\right) - \left(2 \frac{c b_x}{b} + c_x\right) \left(\frac{f'}{\eta}\right)^2 + \frac{g}{\nu^2 c b^4} \left(\frac{\rho_\infty - \rho}{\rho_1}\right) = 0, \tag{17}$$

$$\frac{1}{Pr}\left(\phi'' + \frac{\phi'}{\eta}\right) - \frac{g \beta T}{c_p} \frac{c}{d} \frac{f'}{\eta} + \frac{\nu^2}{c_p} \left(\frac{c^2 b^4}{d}\right) \left(\frac{f''}{\eta} - \frac{f'}{\eta^2}\right)^2 + c_x \frac{f \phi'}{\eta} - \frac{c d_x}{d} \frac{f' \phi}{\eta} = 0, \tag{18}$$

where the subscripts indicate differentiation with respect to x and the primes derivatives with respect to η. The last terms in (15) and (17) are the buoyancy force. Both (16) and (18) contain a term for non-uniform temperature at $y = 0$. The energy effects

of hydrostatic pressure variation and of viscous dissipation are retained in (16) and (18) but will later be neglected.

Similarity requires that the coefficients and buoyancy force in the above equations not be x-dependent. This determines both b and c and the permissible form of d. The specification of the exact form of the local Grashof number, as given below, also determines the buoyancy force term as W/I_w,

$$Gr_x = \frac{gx^3}{\nu^2}\alpha(s_\infty, p)\,|t_0 - t_\infty|^q I_w = \frac{gx^3}{\nu^2}\alpha d^q I_w, \tag{19}$$

$$I_w = \int_0^\infty W d\eta \quad \text{for} \quad R = 0, \quad I_w = \int_0^\infty \phi^q d\eta; \tag{20}$$

where for plane flows

$$b(x) = \tfrac{1}{4}c(x)/x, \quad c(x) = 4(\tfrac{1}{4}Gr_x)^{\frac{1}{4}} \quad \text{and} \quad d = (t_0 - t_\infty) = Nx^n; \tag{21a}$$

and for axisymmetric flows

$$b(x) = \frac{1}{x}(Gr_x)^{\frac{1}{4}}, \quad c(x) = x \quad \text{and} \quad d = (t_0 - t_\infty) = Nx^n. \tag{21b}$$

However, in addition, the buoyancy force may not be x-dependent. From equation (2) we see, if R is not x-dependent, then W is not, assuming that $\phi = \phi(\eta)$. We see from equation (1) that we must have $R = 0$, in the absence of stratification, if $(t_0 - t_\infty)$ is x-dependent, as it is in a developing constant-buoyancy flow. Therefore, we have similarity only for the ambient medium at the extremum temperature corresponding to p and s, i.e. $t_\infty = t_m(s_\infty, p)$.

The downstream temperature decay of any constant-buoyancy flow is determined by the condition that the total convected energy must not vary, even though there is entrainment. The energy per unit transverse span for the two plane flows and the total energy for the axisymmetric plume are, respectively,

$$Q_P(x) = \int_0^\infty \rho c_p (t - t_\infty)\, u\, dy = \rho c_p \nu c d \int_0^\infty \phi f' d\eta \propto x^{\frac{1}{4}(n(q+4)+3)}, \tag{22a}$$

$$Q_A(x) = \int_0^\infty \rho c_p (t - t_\infty)\, u 2\pi y\, dy = 2\pi\mu c_p c d \int_0^\infty \phi f' d\eta \propto x^{n+1}. \tag{22b}$$

Thus there are two values of n for which Q is independent of x:

$$n_P = -3/(q+4) \quad \text{and} \quad n_A = -1. \tag{23}$$

The appearance of $q(s_\infty, p)$ includes the effect of variable ambient salinity and pressure on buoyancy, through the complexity of the density variation with temperature. We note that the corresponding values of n with the conventional Oberbeck–Boussinesq approximation are $-\frac{3}{5}$ and -1, respectively. The values of n in (23) are used in (15) and (17) to determine the downstream temperature decay quantities, N, as

$$N_P = \left[\frac{Q^4}{4^3 g\alpha c_p^4 u^2 \rho^2 I_p^4}\right]^{1/(q+4)} \tag{24a}$$

and

$$N_A = \frac{Q}{2\pi\mu c_p I_A}, \tag{24b}$$

where the following are two values I_P and I_A for the plane and axisymmetric plume, respectively:

$$I_P = I_A = \int_0^\infty f'\phi\, d\eta \equiv I_Q, \tag{25}$$

with the appropriate f' and ϕ for each plume.

With all of these conditions, using equations (15) and (16) with the boundary conditions for the plane plume and line thermal source on an adiabatic surface, equations (13*a*) and (13*b*) become:

$$f''' + \frac{12}{(q+4)} ff'' + \frac{4(q-2)}{(q+4)} f'^2 + \frac{\phi^q}{I_w} = 0, \tag{26}$$

$$\phi'' + \frac{12Pr}{q+4} (f\phi)' = 0;$$

or

$$\phi(\eta) = \exp\left[-\frac{12Pr}{(q+4)} \int_0^\eta f\, d\eta \right], \tag{27}$$

$$\left.\begin{aligned} \phi - 1 = f'' = f = 0 \quad &\text{at} \quad \eta = 0, \\ \phi = f' = 0 \quad &\text{at} \quad \eta \to \infty, \end{aligned}\right\} \tag{28a}$$

$$\left.\begin{aligned} \phi - 1 = f' = f = 0 \quad &\text{at} \quad \eta = 0, \\ \phi = f' = 0 \quad &\text{at} \quad \eta \to \infty. \end{aligned}\right\} \tag{28b}$$

Equations (17), (18) and (13*c*) become for the axisymmetric plume:

$$\frac{f'''}{\eta} + \left(\frac{f-1}{\eta}\right)\left(\frac{f'}{\eta}\right)' + \left(\frac{q-1}{2}\right)\left(\frac{f'}{\eta}\right)^2 + \frac{\phi^q}{I_w} = 0, \tag{29}$$

$$\eta\phi' + Pr f\phi = 0; \tag{30}$$

or

$$\phi(\eta) = \exp\left[-Pr \int_0^\eta (f/\eta)\, d\eta \right],$$

$$f = f' = \phi - 1 = 0 \quad \text{at} \quad \eta = 0, \quad f' = \phi = 0 \quad \text{as} \quad \eta \to \infty. \tag{31}$$

Note that, for $q = 1$, equations (26), (27) and (29), (30) reduce to the 'classical' plume equations. The local mass and momentum convection rates $\dot{m}$ and $\dot{M}$ are, respectively, in the plane and axisymmetric plumes:

$$\dot{m}_P = 4\mu(Gr_x/4)^{\frac{1}{4}} f(\infty), \quad \dot{m}_A = 2\pi\mu x f(\infty), \tag{32a, b}$$

and

$$\dot{M}_P = \frac{4^{\frac{5}{4}}\mu\nu}{x} (Gr_x)^{\frac{3}{4}} \int_0^\infty (f')^2 d\eta, \quad \dot{M}_A = 2\pi\mu\nu (Gr_x)^{\frac{1}{2}} \int_0^\infty (f')^2 d\eta/\eta. \tag{33a, b}$$

The integrals in (33) are referred to as I_M for each plume. The above boundary conditions are optimized for calculation in the sense of Gebhart, Pera & Schorr (1970) and Mollendorf & Gebhart (1974). This produces the simplest and most efficient numerical scheme.

		(a) Plane plume					(b) Line source on adiabatic surface					(c) Axisymmetric plume				
Pr	q	$f'(0)$	$\int_0^\infty w\,d\eta$	$\int_0^\infty f'\phi\,d\eta$	$\int_0^\infty (f')^2 d\eta$	$f(\infty)$	$f''(0)$	$\int_0^\infty w\,d\eta$	$\int_0^\infty f'\phi\,d\eta$	$\int_0^\infty (f')^2 d\eta$	$f(\infty)$	$f''(0)$	$\int_0^\infty w\,d\eta$	$\int_0^\infty f'\phi\,d\eta$	$\int_0^\infty (f')^2 \frac{d\eta}{\eta}$	$f(\infty)$
8·6	1·894816	0·9446	0·2277	0·2685	0·4747	0·8280	0·8565	0·6078	0·1372	0·06813	0·4511	0·8261	0·5010	0·2004	0·5890	3·507
	1·859663	0·9359	0·2303	0·2665	0·4666	0·8212	0·8543	0·6112	0·1368	0·06798	0·4499	0·8189	0·5083	0·2003	0·5794	3·496
	1·727147	0·9042	0·2406	0·2590	0·4375	0·7964	0·8248	0·6248	0·1353	0·06749	0·4454	0·7950	0·5366	0·2001	0·5491	3·456
	1·582950	0·8709	0·2532	0·2512	0·4085	0·7707	0·8357	0·6416	0·1337	0·06709	0·4409	0·7737	0·5698	0·2001	0·5247	3·416
	1·000000	0·7444	0·3284	0·2212	0·3125	0·6787	0·7834	0·7449	0·1272	0·06770	0·4299	0·7168	0·7547	0·2029	0·4977	3·293
9·6	1·894816	0·9499	0·2147	0·2561	0·4747	0·8271	0·8629	0·5837	0·1286	0·06504	0·4429	0·8083	0·4787	0·1804	0·5623	3·504
	1·859663	0·9412	0·2171	0·2542	0·4666	0·8204	0·8609	0·5868	0·1283	0·06491	0·4417	0·8015	0·4856	0·1803	0·5530	3·493
	1·727147	0·9096	0·2268	0·2472	0·4375	0·7955	0·8526	0·5998	0·1269	0·06446	0·4372	0·7791	0·5123	0·1801	0·5236	3·452
	1·582950	0·8765	0·2386	0·2396	0·4085	0·7697	0·8430	0·6157	0·1253	0·06412	0·4328	0·7593	0·5435	0·1801	0·4999	3·411
	1·000000	0·7507	0·3090	0·2112	0·3125	0·6770	0·7924	0·7137	0·1194	0·06487	0·4219	0·7076	0·7174	0·1824	0·4722	3·283
10·6	1·894816	0·9544	0·2036	0·2454	0·4747	0·8265	0·8686	0·5628	0·1213	0·06237	0·4357	0·7925	0·4595	0·1639	0·5394	3·501
	1·859663	0·9458	0·2059	0·2435	0·4666	0·8197	0·8666	0·5658	0·1210	0·06224	0·4354	0·7860	0·4661	0·1639	0·5304	3·490
	1·727147	0·9143	0·2151	0·2368	0·4375	0·7948	0·8586	0·5782	0·1197	0·06184	0·4301	0·7649	0·4914	0·1637	0 5018	3·449
	1·582950	0·8813	0·2262	0·2297	0·4085	0·7688	0·8494	0·5934	0·1182	0·06153	0·4257	0·7463	0·5210	0·1637	0·4787	3·408
	1·000000	0·7563	0·2926	0·2024	0·3125	0·6757	0·8003	0·6869	0·1127	0·06239	0·4148	0·6990	0·6856	0·1657	0·4506	3·275
11·6	1·894816	0·9584	0·1941	0·2359	0·4747	0·8259	0·8736	0·5445	0·1150	0·06001	0·4292	0·7782	0·4429	0·1503	0·5194	3·499
	1·859663	0·9499	0·1963	0·2342	0·4666	0·8191	0·8716	0·5475	0·1147	0·05989	0·4280	0·7721	0·4491	0·1502	0·5107	3·488
	1·727147	0·9184	0·2049	0·2277	0·4375	0·7941	0·8639	0·5593	0·1134	0·05952	0·4237	0·7520	0·4733	0·1500	0·4829	3·447
	1·582950	0·8856	0·2155	0·2208	0·4085	0·7682	0·8549	0·5739	0·1121	0·05925	0·4194	0·7344	0·5015	0·1500	0·4604	3·405
	1·000000	0·7612	0·2785	0·1947	0·3125	0·6746	0·8074	0·6635	0·1069	0·06020	0·4085	0·6911	0·6581	0·1518	0·4320	3·268
12·6	1·894816	0·9620	0·1857	0·2275	0·4747	0·8254	0·8780	0·5284	0·1094	0·05791	0·4234	0·7652	0·4281	0·1387	0·5019	3·498
	1·859663	0·9534	0·1878	0·2258	0·4666	0·8186	0·8761	0·5312	0·1091	0·05781	0·4222	0·7593	0·4341	0·1386	0·4933	3·486
	1·727147	0·9221	0·1961	0·2196	0·4375	0·7936	0·8686	0·5426	0·1080	0·05747	0·4179	0·7402	0·4573	0·1385	0·4662	3·444
	1·582950	0·8894	0·2062	0·2130	0·4085	0·7676	0·8599	0·5566	0·1067	0·05722	0·4137	0·7236	0·4842	0·1385	0·4442	3·402
	1·000000	0·7655	0·2661	0·1879	0·3125	0·6737	0·8136	0·6429	0·1019	0·05824	0·4029	0·6836	0·6340	0·1401	0 4156	3·263
13·6	1·894816	0·9652	0·1784	0·2199	0·4747	0·8250	0·8819	0·5139	0·1045	0·05603	0·4180	0·7532	0·4150	0·1287	0·4862	3·496
	1·859663	0·9567	0·1803	0·2183	0·4666	0·8182	0·8801	0·5166	0·1042	0·05593	0·4169	0·7476	0·4207	0·1287	0·4779	3·485
	1·727147	0·9254	0·1883	0·2123	0·4375	0·7931	0·8729	0·5276	0·1031	0·05562	0·4127	0·7294	0·4430	0·1286	0·4514	3·443
	1·582950	0·8928	0·1979	0·2059	0·4085	0·7671	0·8644	0·5412	0·1020	0·05540	0·4085	0·7136	0·4690	0·1285	0·4299	3·399
	1·000000	0·7694	0·2553	0·1817	0·3125	0·6729	0·8193	0·6245	0·09738	0·05647	0·3977	0·6767	0·6126	0·1300	0·4012	3·258

TABLE 1. Calculated flow and transport quantities for various flow configurations and values of Pr and q as indicated. Note that rounding q from seven to four significant digits will result in an error of less than 0·1 % in the calculated results. See text for further discussion.

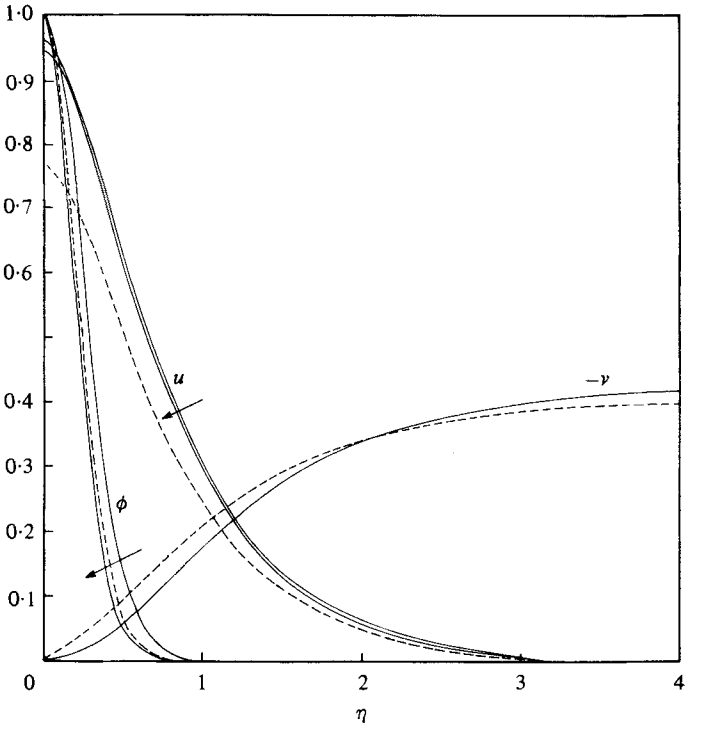

FIGURE 1. Calculated velocity and temperature fields for a freely rising plane plume for $q = q(0, 1) = 1{\cdot}894816$. Dashed lines are conventional Oberbeck–Boussinesq results, i.e. $q = 1$ for $Pr = 12{\cdot}6$. Arrows indicate increasing Pr: 8·6 and 12·6. The Prandtl number effect on $-v$ is indistinguishable on this figure. Note that rounding q from seven to four significant digits will result in an error of less than 0·1% in the calculated results. See text for further discussion.

3. Calculated results

Equations and boundary conditions (26)–(31) were numerically integrated on a CDC 6400 using a fourth-order double-precision predictor–corrector scheme and a standard shooting method incorporating a Newton–Raphson correction technique for guessed boundary conditions. Automatic local subdivision of the independent variable for prescribed accuracy levels was used. Integration was performed outward for a successively smaller accuracy criterion, from $\eta = 0$ to sufficiently large values of η to ensure the accuracy implied by the number of digits given here. Calculated numerical results are given in table 1 for $Pr = 8{\cdot}6$, 9·6, 10·6, 11·6, 12·6 and 13·6 and for five values of q ranging from about $q = 1{\cdot}895$ to $q = 1$ for each of the three flows. The condition $q = 1$, for each Pr, corresponds to results which amount to the conventional Oberbeck–Boussinesq approximation of a linear dependence of density on temperature. Other values of q correspond to various values of ambient salinity and pressure.

We have retained for the calculations the full value of q for accuracy. Rounding q from 1·894816 to 1·90 produces about a 0·2% error in the units of buoyancy for the plane plume. After discussing the results of the calculations we shall estimate the effect on overall transport parameters of rounding q. It will be shown later that,

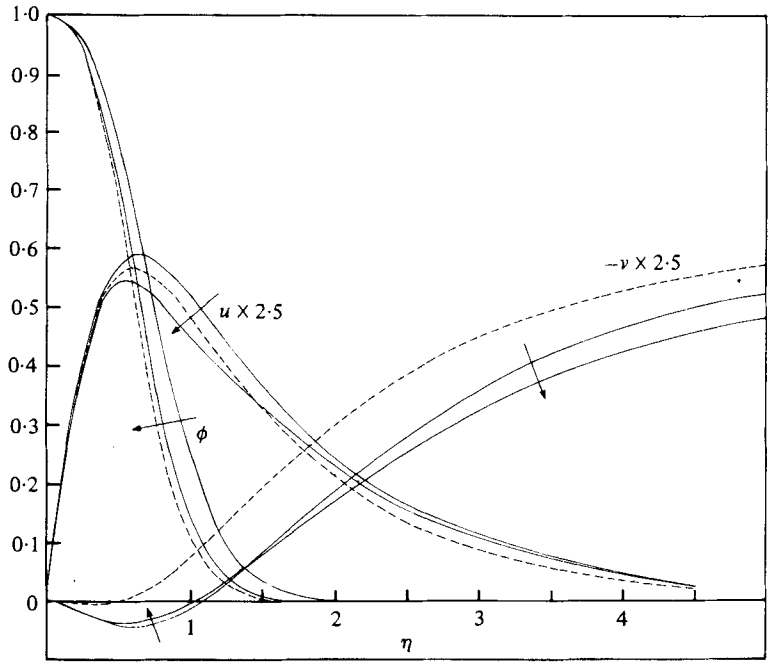

FIGURE 2. Calculated velocity and temperature fields for a thermal line source on an adiabatic surface for $q = q(0, 1) = 1{\cdot}894816$. Dashed lines are conventional Oberbeck–Boussinesq results, i.e. $q = 1$ for $Pr = 12{\cdot}6$. Arrows indicate increasing Pr: 8·6 and 12·6. Note that rounding q from seven to four significant digits will result in an error of less than 0·1 % in the calculated results. See text for further discussion.

although precise values are used for calculations, q may be rounded to four digits with an attendant error of less than 0·1 % in calculated transport quantities.

The velocity and temperature fields for a freely rising plane plume are shown in figure 1 for $q = q(0, 1) = 1{\cdot}894816$ and for values of Prandtl number 8·6 and 12·6. This range of Pr is applicable to most cold water situations. Oberbeck–Boussinesq results are shown as dashed lines for $Pr = 12{\cdot}6$. The most pronounced effect of a density extremum is seen to be an increase of more than 20 % in the upward axial velocity component near the plume centre-plane. There is a corresponding adjustment in the horizontal velocity component. Density-extrema effects on the temperature field are much less pronounced.

Figure 2 shows the velocity and temperature profiles for a line source of heat on a vertical adiabatic surface. The flow behaviour is seen to be very different from that of the freely rising plume. This is a result of a high-shear region introduced by the presence of the surface. The most striking density-extrema effect is in the horizontal velocity component. In general, because of fluid entrained into the primary upward flow there is a net increase in the local mass flow in the plume with downstream distance. For most buoyancy-induced flows, the entrainment or horizontal fluid velocity is inward ($v < 0$) over the entire flow region. However, it is known that a reversal in direction in the horizontal velocity component occurs for some flows. For example, such a trend was indicated by Mollendorf & Gebhart (1973) in a study of round laminar jets. A consequence of this is the appearance, in the flow region, of a location of vanishing v velocity. This is most clearly seen from the closed-form solution

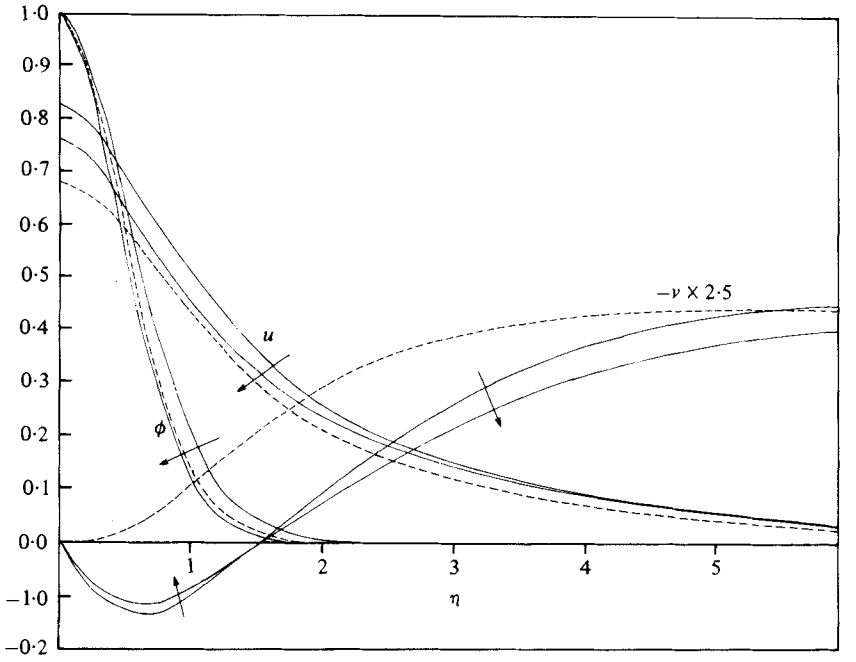

FIGURE 3. Calculated velocity and temperature fields for a freely rising axisymmetric plume for $q = q(0, 1) = 1{\cdot}894816$. Dashed lines are conventional Oberbeck–Boussinesq results, i.e. $q = 1$ for $Pr = 12{\cdot}6$. Arrows indicate increasing Pr: 8·6 and 12·6. Note that rounding q from seven to four significant digits will result in an error of less than 0·1 % in the calculated results. See text for further discussion.

for a round laminar jet. Such a reversal in the v component of velocity is also found here in the flow above a line source on an adiabatic surface. Again, the dashed lines indicate conventional Oberbeck–Boussinesq results, for which a relatively weak reversal in the v component of velocity is seen. An asymptotic expansion for v about $\eta = 0$ for $q = 1$, $v \sim (\nu/x)(\frac{1}{4}Gr_x)^{\frac{1}{4}}[f''(0) - \eta](\eta^2/10) + \ldots$, also indicates the presence of such a reversal. Density extrema effects are seen to accentuate this effect but otherwise to cause relatively minor alterations to the velocity and temperature fields.

Similarly, figure 3 shows the calculated velocity and temperature profiles for a freely rising axisymmetric plume. Except for the pronounced alteration of entrainment velocity, the trends are similar to those of a plane plume. Density extrema effects are seen to result in a striking reversal in the direction of the v component of velocity near the plume axis. This effect is much stronger for the axisymmetric plume than for the plane wall plume.

The variation of the local buoyancy force, ϕ^q/I_w, is shown in figure 4 for the three plumes considered here. The trends of density-extrema effects are seen to be the same for each flow shown. Near the axis of the plumes, there is an increase in buoyancy force beyond that of conventional Oberbeck–Boussinesq results. A decrease is seen near the edge of the flow region.

Also of interest is the mass flow rate, maximum velocity and, for the plane wall plume, the surface shear. The variation of these quantities with Pr and q are tabulated in table 1 for the plane, wall and axisymmetric plumes. Note that for the axisymmetric plume the maximum velocity is $f''(0)$, whereas for the freely rising plane plume it is

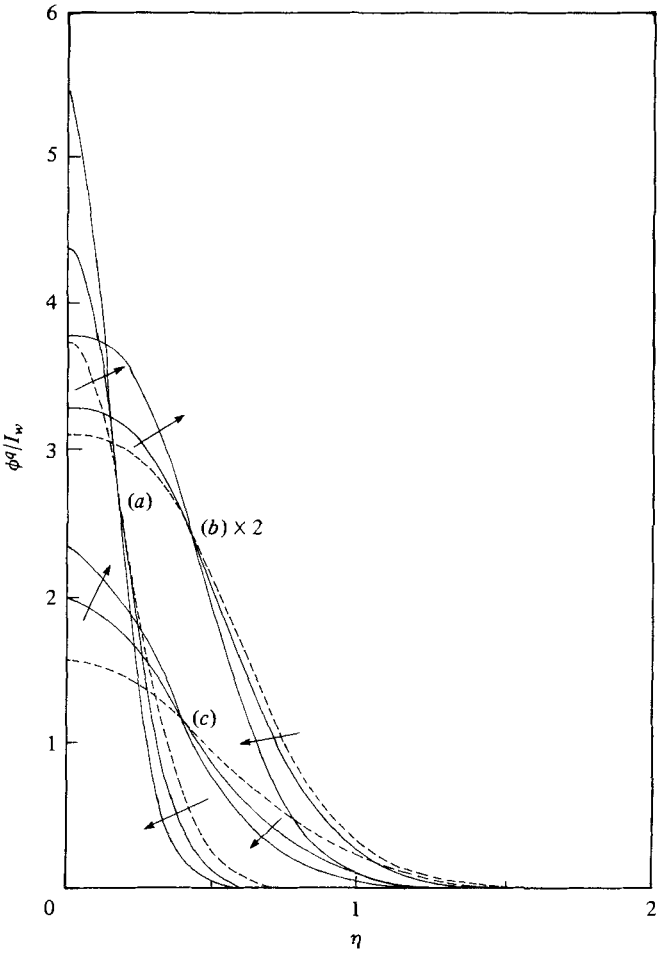

FIGURE 4. Distribution of local buoyancy force, ϕ^q/I_w, for (*a*) plane plume, (*b*) line source on an adiabatic surface and (*c*) axisymmetric plume. Dashed lines are conventional Oberbeck–Boussinesq results, i.e. $q = 1$ for Pr: 8·6 and 12·6. Arrows indicate increasing Pr: 8·6 and 12·6. Note that rounding q from seven to four digits will result in an error of less than 0·1 % in the calculated results. See text for further discussion.

$f'(0)$. The Prandtl-number range considered is from 8·6 to 13·6 for $1 \leqslant q \leqslant 1{\cdot}895$. Again the condition $q = 1$ corresponds to conventional Oberbeck–Boussinesq results with other values of q corresponding to other values of ambient salinity and pressure. Except for the wall plume, there is a relatively weak Pr effect on mass flow rate. There is, however, a significant q effect on the mass flow rate over the range of Pr considered. For each plume, density extrema effects are seen to increase the mass flow. There is a corresponding increase in the maximum of the upward velocity component for both the freely rising plane and axisymmetric plume. An increase in surface shear, with increasing q, is seen in table 1 for the wall plume.

Table 1 shows the Pr and q variation of the integrated buoyancy force, convected heat and momentum flux, i.e. I_w, I_Q and I_M, respectively. Table 1 also shows that I_w increases with Pr and q for each of the three plumes. Density-extrema effects are seen to decrease I_w significantly, as does increasing Pr. There is a corresponding increase

in I_Q for the plane freely rising and wall plumes. A decrease in I_Q, with increasing q and Pr, is seen in table 1, for the axisymmetric plume. The momentum flux integral, I_M, is increased by density-extrema effects for both the freely rising plumes, but not for the wall plume.

Throughout the foregoing calculations we have used the precise numerical values of q which relate to the easily identifiable conditions $q(0, 1)$, $q(0, 100)$, $q(0, 500)$ and $q(0, 1000)$. The summarized results in table 1 are then very accurate for these specific conditions, for any subsequent uses which may arise. Here we use these results to estimate the effects of rounding q up or down from these precise numerical values. The effect of q is seen to be about the same for each flow represented in table 1. Certainly I_w is the most sensitive of the transport parameters. The results in table 1, for the plane plume, indicate that I_w increases by about 1 part per two parts decrease in $q(s, p)$. As a result, a change in I_w of 0·1 % accompanies a change in the value of q of about 0·0035. Thus, for example, $q(0, 500) = 1{\cdot}727\,147$ may be rounded to 1·727 without affecting accuracy to 0·1 % in I_w.

4. Conclusions

Unlike conventional Oberbeck–Boussinesq results, the inclusion of density-extrema effects in ambient unstratified cold-water precludes the existence of similarity solutions for the freely rising plane, axisymmetric and wall plumes, unless the ambient temperature is at $t_m(s_\infty, p_\infty)$. For this condition, the flow is always vertically upward regardless of whether the flow originates from a source or sink of thermal energy. The calculated results for these flows presented here, cover a very wide range of ambient temperature, salinity and pressure conditions. Saline diffusion is not considered inasmuch as the Sorét and Dufort effects are not significant for these flows. The effect of variable ambient salinity and pressure has, however, been included through the parameters $q(s_\infty, p_\infty)$, $t_m(s_\infty, p_\infty)$ and $\alpha(s_\infty, p_\infty)$. In addition, the temperature level influences the Prandtl number, $Pr = Pr(t_\infty, s_\infty, p_\infty)$, as well as other fluid properties.

Several important findings are presented here. Conventional Oberbeck–Boussinesq results incorporate a linear dependence of density on temperature and do not accurately represent density-extrema effects. The present analysis uses a new, simple and accurate equation of state for pure and saline water. Instead of ϕ, the buoyancy force becomes ϕ^q. In addition, the coefficients in the governing equations depend on q. Density extrema effects also modify the x dependence of the flow and transport quantities. A comparison of presently determined and conventional x dependence of the various flow and transport quantities is shown in table 2 for each plume. Note that q may take on values between about 1·6 and 1·9 depending on the ambient salinity and pressure. Conventional Oberbeck–Boussinesq results correspond to $q = 1$. Table 2 shows that the x-dependence of u is altered the most by density-extrema effects. For plane plumes it goes from $x^{0\cdot200}$ to $x^{0\cdot018}$ or $x^{0\cdot075}$, depending on q. For axisymmetric plumes it goes from being independent of x to $x^{-0\cdot447}$ or $x^{-0\cdot291}$, depending on q. The density extrema effects for the other quantities in table 2 are significant but not as pronounced as for u. Hence, the dependence of density on temperature has a striking influence on the downstream behaviour of transport, compared to conventional Oberbeck–Boussinesq results, as well as to cause large changes in the magnitude of flow and transport quantities at a given downstream location.

	Plane plumes		Axisymmetric plume	
	OB	Present	OB	Present
u	$\frac{1}{5}$	$(2-q)/(4+q)$	0	$\frac{1}{2}(1-q)$
v	$-\frac{2}{5}$	$-(q+1)/(q+4)$	$-\frac{1}{2}$	$-\frac{1}{4}(q+1)$
t_0-t_∞	$-\frac{3}{5}$	$-3/(q+4)$	-1	-1
$\dot{m}$	$\frac{3}{5}$	$3/(q+4)$	1	1
$\dot{M}$	$\frac{4}{5}$	$(5-q)/(4+q)$	1	$\frac{1}{2}(3-q)$

TABLE 2. A comparison of conventional Oberbeck–Boussinesq (OB) and the presently determined x dependence of the various flow and transport quantities for each plume. The entries in the table are exponents of the downstream distance, x.

The authors acknowledge support for this study by the National Science Foundation under research grants GK18529, ENG75-05466 and ENG75-22623 (B. G.) and ENG76-16936 (J.C.M.). The many helpful suggestions of the referees are also gratefully acknowledged.

REFERENCES

BENDELL, M. S. & GEBHART, B. 1976 Heat transfer and ice-melting in ambient water near its density extremum. *Int. J. Heat Mass Transfer* **19**, 1081–1087.

CALDWELL, D. R. 1974 Experimental studies on the onset of thermohaline convection. *J. Fluid Mech.* **64**, 347–367.

CHEN, C. T. & MILLERO, F. J. 1976 The specific volume of sea water at high pressures. *Deep-Sea Res.* **23**, 595–612.

FINE, R. A. & MILLERO, F. J. 1973 Compressibility of water as a function of temperature and pressure. *J. Chem. Phys.* **59**, 5529–5536.

GEBHART, B. 1971 *Heat Transfer*, 2nd edn. McGraw-Hill.

GEBHART, B. 1973 Boundary layer flows and instability in natural convection. *Adv. Heat Transfer* **9**, 273–348.

GEBHART, B. & MOLLENDORF, J. C. 1977 A new density relation for pure and saline water. *Deep-Sea Res.* **24**, 831–848.

GEBHART, B. & MOLLENDORF, J. C. 1978 Buoyancy-induced flows in water under conditions in which density extrema may arise. *J. Fluid Mech.* **89**, 673–707.

GEBHART, B. & PERA, L. 1971 The nature of vertical natural convection flows resulting from the combined buoyancy effects of thermal and mass diffusion. *Int. J. Heat Mass Transfer* **14**, 2025–2050.

GEBHART, B., PERA, L. & SCHORR, A. W. 1970 Steady laminar natural convection plumes above a horizontal line heat source. *Int. J. Heat Mass Transfer* **13**, 161–171.

MERK, H. J. 1953 The influence of melting and anomalous expansion on the thermal convection in laminar boundary layers. *Appl. Sci. Res.* **4**, 435–452.

MOLLENDORF, J. C. & GEBHART, B. 1973 Thermal buoyancy in round laminar vertical jets. *Int. J. Heat Mass Transfer* **16**, 735–745.

MOLLENDORF, J. C. & GEBHART, B. 1974 Axisymmetric natural convection flows resulting from the combined buoyancy effects of thermal and mass diffusion. *Proc. 5th Int. Heat Transfer Conf., Tokyo.*

PERA, L. & GEBHART, B. 1972 Natural convection flows adjacent to horizontal surfaces resulting from the combined effects of thermal and mass diffusion. *Int. J. Heat Mass Transfer* **15**, 269–278.